Title

Cellular positioning and dendritic field size of cholinergic amacrine cells are impervious to early ablation of neighboring cells in the mouse retina

Journal

Visual Neuroscience, 21(1)

ISSN

0952-5238

Authors

Farajian, R
Raven, M A
Cusato, K
et al.

Publication Date

2004

Peer reviewed

Visual Neuroscience (2004), **21**, 13–22. Printed in the USA.

DOI: 10.1017/S0952523807041026

Cellular positioning and dendritic field size of cholinergic amacrine cells are impervious to early ablation of neighboring cells in the mouse retina

REZA FARAJIAN, MARY A. RAVEN, KAREN CUSATO, AND BENJAMIN E. REESE

Neuroscience Research Institute and Department of Psychology, University of California at Santa Barbara, Santa Barbara

(RECEIVED October 23, 2003; ACCEPTED December 5, 2003)

Abstract

We have examined the role of neighbor relationships between cholinergic amacrine cells upon their positioning and dendritic field size by producing partial ablations of this population of cells during early development. We first determined the effectiveness of L-glutamate as an excitotoxin for ablating cholinergic amacrine cells in the developing mouse retina. Subcutaneous injections (4 mg/g) made on P-3 and thereafter were found to produce a near-complete elimination, while injections at P-2 were ineffective. Lower doses on P-3 produced only partial reductions, and were subsequently used to examine the effect of partial ablation upon mosaic organization and dendritic growth of the remaining cells. Four different Voronoi-based measures of mosaic geometry were examined in L-glutamate-treated and normal (saline-treated) retinas. Partial depletions of around 40% produced cholinergic mosaics that, when scaled for density, approximated the mosaic geometry of the normal retina. Separate comparisons simulating a 40% random deletion of the normal retina produced mosaics that were no different from those experimentally depleted retinas. Consequently, no evidence was found for positional regulation in the absence of normal neighbor relationships. Single cells in the ganglion cell layer were intracellularly filled with Lucifer Yellow to examine the morphology and dendritic field extent following partial ablation of the cholinergic amacrine cells. No discernable effect was found on their starburst morphology, and total dendritic field area, number of primary dendrites, and branch frequency were not significantly different. Cholinergic amacrine cells normally increase their dendritic field area after P-3 in excess of retinal expansion; despite this, the present results show that this growth is not controlled by the density of neighboring processes.

Keywords: Excitotoxicity, Glutamate, Plasticity, Morphology, Regularity, Stratification, Coverage factor

Introduction

Individual types of retinal neurons are distributed across the retinal surface to provide a uniform sampling of the visual field (Wässle & Riemann, 1978). This organization is achieved by mechanisms operating during development that distribute cells of a particular type into a regular array, and that establish the size and morphology of the dendritic field. By virtue of their regularity and their generally symmetrical dendritic fields, each type of neuron provides a relatively uniform "dendritic coverage" of the retina. This dendritic coverage is defined by the extent to which the dendrites of adjacent cells overlap, expressed as the "coverage factor," being the product of dendritic field area and cell density. Different cell types exhibit differing degrees of dendritic coverage. For example, ON and OFF beta ganglion cells in the cat retina have coverage factors around 3.0, while ON and OFF alpha cells have coverage factors closer to 1.0, their dendrites extending just beyond the limits of the dendritic field of neighboring cells (Wässle et al., 1981*a*,*b*). There is no close correspondence between cell density, regularity, and dendritic field size, as cell types that have comparable densities can have conspicuously different dendritic field areas (and consequently, different coverage factors) as well as regularity indexes. In the mouse retina, for example, the horizontal cells and ON and OFF cholinergic amacrine cells have comparable densities (1500–1700 cells per mm^2; Strettoi & Volpini, 2002), while the dendritic field diameter of a cholinergic amacrine cell is roughly three times that of a horizontal cell (He et al., 2000; Badea et al., 2003). The regularity index (nearest-neighbor distance/standard deviation) for horizontal cells is around 5.0, while that for cholinergic amacrine cells is around 3.5 (Galli-Resta et al., 2000; Raven & Reese, 2002).

The factors governing dendritic outgrowth, field size, and morphology are controlled by cell-intrinsic programs associated with the realization of cellular fate, but are also believed to involve interactions with neighboring cells. The dendritic structure of retinal ganglion cells is perhaps the most throughly studied with

Address correspondence and reprint requests to: Benjamin E. Reese, Neuroscience Research Institute, University of California at Santa Barbara, Santa Barbara, CA 93106-5060, USA. E-mail: breese@psych.ucsb.edu

respect to environmental dependency: alpha and beta cells both show redirected growth of their dendrites when neighboring cells of the same type are eliminated during early development (Perry & Linden, 1982; Eysel et al., 1985). One factor controlling this dendritic growth is believed to be a competition-based interaction for afferents (Linden & Perry, 1982) mediated *via* activity-dependent mechanisms (Deplano et al., 1999; see also Lohmann et al., 2002; Wong & Ghosh, 2002). Such interactions may occur directly through a contact-mediated mechanism, since such like-type cells show specificity in their contacts with one another during the period of dendritic growth (Lohmann & Wong, 2001). Interactions between different types of retinal ganglion cells have also been found (Ault et al., 1993), and certain ganglion and amacrine cell classes exhibit cross-type specificity in their contacts during development (Stacy & Wong, 2003).

Contact-mediated repulsion between like-type cells has also been proposed to control their intercellular spacing during development, driving neighboring cells to move apart from one another (Eglen et al., 2000; Reese & Galli-Resta, 2002). Cholinergic amacrine cells disperse tangentially within the retina during the period when new cholinergic amacrine cells are being inserted into their developing mosaic (Galli-Resta et al., 1997). When microtubule stability is disrupted in immature cholinergic amacrine cells, the regularity of their mosaic transiently collapses until stability is re-achieved (Galli-Resta et al., 2002). Indeed, a tensile interaction between cholinergic amacrine cells, mediated possibly through cadherin expression on their dendrites (Honjo et al., 2000), may be responsible for their intercellular spacing (Galli-Resta, 2002). Cholinergic amacrine cells are wide-field neurons that stratify in one of two layers within the inner plexiform layer (IPL). Because of their dendritic extent, these neurons typically exhibit dendritic coverage factors far in excess of the other neurons mentioned above, ranging from 10 to 70 depending on the species (Tauchi & Masland, 1984; Vaney, 1984; Schmidt et al., 1985; Voigt, 1986; Rodieck & Marshak, 1992; Sandmann et al., 1997). How these cells regulate their dendritic extent, as well as their positioning, is unclear, but their density and dendritic field size should permit ample opportunity for interactions with neighboring cells during development.

The present investigation has sought to produce partial ablations of cholinergic amacrine cells during early development in order to examine the consequence of their local reduction upon the positioning and dendritic field extent of remaining cells. We have used a pharmacological approach, employing L-glutamate as an excitotoxin (Fischer et al., 1998; Reese et al., 2001; Johnson et al., 2001). The latter, used in the developing ferret and chick, and more recently in the developing mouse (Park et al., 2002), confers its selectivity by virtue of the differential expression of ionotropic glutamate receptors upon retinal neurons during early development (Marc, 1999*a*,*b*). Its specificity has been described in the ferret, and there, a few additional cell types are compromised, but the cholinergic amacrine cells were found to be maximally sensitive to its excitotoxic effect (Reese et al., 2001; Johnson et al., 2001). A preliminary report of comparable results from the developing rat retina has also recently appeared (Chun et al., 2001). We first describe this excitotoxic approach for cholinergic amacrine cell depletion in the mouse retina, documenting the time-course, dose dependency, and cell specificity following exposure to L-glutamate during the perinatal period. We then report the effects of this depletion upon the mosaic order of the remaining population of cholinergic amacrine cells. Finally, we describe the consequences of this partial depletion upon the morphology of single, intracellularly filled, cholinergic amacrine cells.

Materials and methods

Male and female C57BL/6 mice were bred in the UCSB central vivarium from stock originally obtained from Charles River Laboratories, with the day of birth being designated postnatal day (P) 1. A single dose of L-glutamate, dissolved in H_2O using sodium hydroxide and then adjusted to physiological pH, was injected subcutaneously on either P-2, P-3, P-4, or P-6, at either 1.3, 2.6, or 4.0 mg/g of body weight, to the entire litter. Control animals were treated identically, but were given saline vehicle without the L-glutamate. Mice were then reared until 3 weeks of age, when they were euthanized with a lethal dose of sodium pentobarbital (120 mg/kg, i.p.) followed by intracardial perfusion using 0.9% saline and then 4% paraformaldehyde in 0.1 M sodium phosphate buffer (pH 7.2 at 20°C). Alternatively, mice used for single-cell injections were reared until 1–3 months of age, and then euthanized with the same dose of sodium pentobarbital. All procedures were conducted under authorization by the UCSB Institutional Animal Care and Use Committee, and in accord with the NIH Guide for the Care and Use of Laboratory Animals.

Immunolabeling

The retinas from fixed eyes were either dissected immediately and prepared for wholemount immunofluoresence or immunohistochemistry, or the posterior eyecup was embedded in gelatin and sectioned at 16 μm in a plane passing radially through the optic nerve head. Ten adjacent one-in-ten series were mounted and processed for immunohistochemistry. These procedures were identical to those previously described for mouse retina (Reese et al., 1999). Primary antibodies included a goat polyclonal choline acetyltransferase antibody (ChAT; 1:50; Chemicon; Temecula, CA); a mouse monoclonal antibody to tyrosine hydroxylase (TH; 1:10,000; Sigma; St. Louis, MO); a mouse monoclonal antibody to calbindin-D28 (calb; 1:10,000; Sigma); a mouse monoclonal antibody to protein kinase C (PKC; 1:50; Amersham; Piscataway, NJ); a rabbit polyclonal antibody to gamma-aminobutyric acid (GABA: 1:10,000; Sigma); a rabbit polyclonal antibody to neurofilaments (NF-150; 1:1000; Chemicon); and a goat polyclonal antiserum to the glycine transporter 1 (GlyT1; 1:10,000; Chemicon). Primary antibodies were detected using either biotinylated IgGs followed by streptavidin conjugated to horseradish peroxidase (HRP; Biomeda; Foster City, CA, or Elite Vectorstain kits; Burlingame, CA) or to Alexa 488 (Molecular Probes; Eugene, OR) or Cy2 (Jackson ImmunoResearch; West Grove, PA), or using IgGs conjugated to Texas Red or Cy2 (Jackson ImmunoResearch). An adjacent series of sections was processed as a negative control, in which phosphate buffer was substituted for the primary antibody, while another was always stained with either cresyl violet or 4′-6-diamidino-2-phenylindole hydrochloride (DAPI) to reveal the architecture of the retina.

Single-cell filling

Retinas for single-cell injection were dissected from the eyecups in 2% paraformaldehyde and 0.01% glutaraldehyde in 0.1 M sodium phosphate buffer and then postfixed as wholemounts for a total duration in fixative for ~30 min. They were subsequently mounted on clean slides, incubated in 2.9×10^{-5} M DAPI for 5 min, then maintained in a bath of phosphate buffer with 2 mM ascorbic acid, and viewed on a Nikon Eclipse E600FN fixed-stage microscope equipped for fluorescense and differential interference contrast

(DIC) microscopy, all at 20°C. Small neurons in the ganglion cell layer (GCL) were impaled using sharp micropipettes drawn to a tip of ~0.5–1.0 μm. Pipettes were filled with 2% Lucifer Yellow CH (Molecular Probes), and ~2-5 nA negative current was passed for roughly 10–20 min until the morphology of cholinergic amacrine cells was clearly revealed. Filling of non-cholinergic cells was usually aborted immediately. For these experiments, treated retinas were compared with normal mouse retinas of comparable age rather than saline-treated control retinas. Filled cells were either photographed using an Olympus BHS fluorescence microscope or using a Bio-Rad (model 1024) laser scanning confocal microscope. A subset of the retinas were also immunostained using a rabbit polyclonal antibody to Lucifer Yellow (1:100; Chemicon) and the above antibody to ChAT in order to compare dendritic morphology with the pattern of local depletion of cholinergic amacrine cells. As previously noted, the immunoreactivity of injected cells was compromised by the Lucifer Yellow (Voigt, 1986; He et al., 2000).

Analysis of cell densities, retinal area, and soma size

The density of different cell types was determined either in wholemount preparations or in sectioned material. In retinal wholemounts, sample fields were obtained using a 20× objective at 1-mm intervals across the retinal surface in a square grid, yielding 10–13 samples per retina (horizontal and cholinergic amacrine cells), or two sample fields near the optic nerve head were analyzed (dopaminergic amacrine cells). Labelled cells were counted and converted to cells/mm^2, and an average density per retina was then obtained, with a minimum of three retinas per condition being analyzed. Retinal areas were also measured in these wholemounted retinas. Cholinergic soma areas were also measured from 35 adjacent cells in the GCL in each of three saline-treated control retinas and three retinas that had been exposed to 2.6 mg/g L-glutamate on P-3. All fields for soma size analysis were sampled at a location midway between the retinal periphery and optic nerve head in wholemount preparations, yielding a total sample of 105 cells in each condition. In sectioned material, linear densities of particular cell types were determined by counting cells in three sections centered on, or immediately adjacent to, the optic nerve head, and then dividing the total number of cells by the length of sampled retina. All of these procedures have been described elsewhere (Reese et al., 2001; Raven & Reese, 2002).

Analysis of mosaic organization

From those same samples of wholemounted retinae immunostained for ChAT, the *X*–*Y* coordinates for the position of each cholinergic amacrine cell in the GCL were identified, and from these, the geometric properties of the mosaic were analyzed using four Voronoi-based measures: Delaunay segment length, Delaunay area, nearest-neighbor distance, and Voronoi domain area. These were determined for each field, and an average frequency distribution was generated from all of the fields for each animal. Distributions for individual animals were plotted, permitting an appreciation of interindividual variability in both the control and treated conditions. To compare directly the geometry of these mosaics independent of their density differences, each of the distributions was scaled by the ratio of cholinergic cell density (or, for the linear measures, by the square root of that ratio) in a depleted GCL mosaic to the average cholinergic cell density in the normal control GCL mosaics. Simulations were also prepared in which we randomly deleted 40% of the cells in each of the sample fields for three of the control retinas, for direct comparison with the experimental depletions that averaged 40%, using a customized program for this purpose (Rossi et al., 2003).

Analysis of dendritic fields

Filled cells in the GCL were examined on an Olympus BHS fluorescence microscope equipped with a video camera and *X*–*Y* stage encoders linked to a computer running Bioquant Topographer Nova Prime software (R & M Biometrics; Nashville, TN). The entire retinal area was outlined, and the position of each filled cell was identified. Using a 40× objective, the full extent of the dendritic field was traced, as was the inner boundary defined by the annulus of varicosities positioned upon the distal dendrites (Famiglietti, 1983; Wong & Collin, 1989), associated with the synaptic output of these cells (Famiglietti, 1991). From these measurements, each cholinergic amacrine cell's eccentricity (relative to the optic nerve head), total dendritic field area, and inner and outer (annular) dendritic field areas were determined, from a total of 14 cells from L-glutamate-treated retinas and 26 cells from normal retinas. A subset of these cells were also used to determine the number of radiating primary dendrites, and the number of branch points distal to the primary dendrite. As the number of primary dendrites so analyzed varied between cells, an average for each cell was generated, from which an average per condition was generated.

Results

Excitotoxic effects of L-glutamate in the mouse retina

A single subcutaneous dose of 4 mg/g L-glutamate was found to produce a substantial reduction in the size of the cholinergic amacrine cell population, shown here in wholemount preparations focused on the GCL (Fig. 1a). There was a sensitive period for this effect, with injection of L-glutamate being without any effect on P-2, yet producing a near-complete ablation of these cells on either P-4 or P-6 (Fig. 1b). To examine the selectivity of this effect, retinas from these same ages were either immunostained for calbindin D-28, to label the horizontal cells, or for tyrosine hydroxylase, to label the dopaminergic amacrine cells. In each of those cases, the number of cells was unaffected by L-glutamate treatment (Figs. 1c and 1d). Total retinal area was slightly reduced by the L-glutamate at P-4 and P-6 (Fig. 1e), but as these animals appeared slightly smaller than age-matched control litters, this is unlikely to reflect any specific stunting of retinal areal growth.

These results suggest that P-3 should be the onset of sensitivity for the excitotoxic effects of L-glutamate. The dose of L-glutamate was therefore varied on P-3 to find the earliest possible time when we could produce partial ablation of the cholinergic amacrine cell population. The same dose of L-glutamate (4 mg/g) produced a near-complete loss of cholinergic amacrine cells, as on P-4 and P-6, suggesting that the onset of sensitivity is a rapid one, while lower doses (1.3 and 2.6 mg/g) were found to produce intermediate levels of depletion (Fig. 1f). Measurements of soma area for surviving cholinergic amacrine cells indicated no reduction in size, suggesting that the sublethal exposure to L-glutamate had not compromised the maturation of these surviving cells (Fig. 1g). We settled on a dose of 2.6 mg/g, administered on P-3, as a means of producing a partial reduction of the cholinergic amacrine cell population.

Counterstained sections of such L-glutamate-treated retinas indicated that retinal histology was largely normal (Fig. 1h): three distinct cellular layers were detected, separated by two plexiform layers, although the inner retina appeared thinner, particularly the IPL. The stratification of the IPL appeared relatively normal, but for the loss or reduction in density of the cholinergic strata (Fig. 1i, top). The distribution of the dopaminergic processes, the rod bipolar terminals, and the glycinergic processes were all largely unchanged (Figs. 1i & 1j). Immunostaining for GABA revealed a lighter distribution across the thickness of the IPL (Fig. 1k, top). Horizontal cell processes within the outer nuclear layer (ONL) were normally stratifying, although occasional processes were misdirected into the inner retina (not shown), as previously reported (Park et al., 2002).

At a dose of 2.6 mg/g, L-glutamate near completely abolished the outer stratum of cholinergic processes within the IPL, while

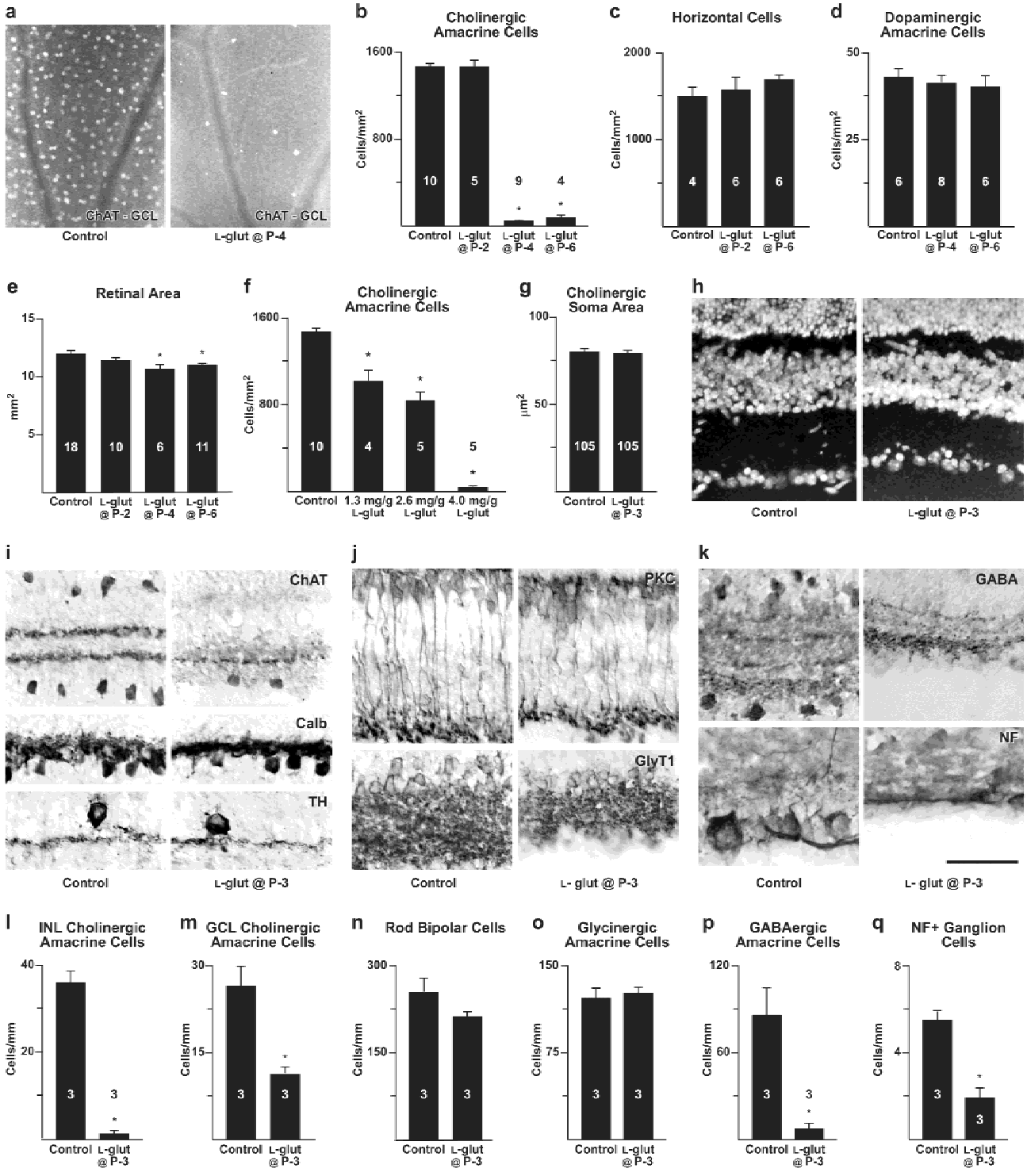

only reducing the density of the inner stratum (Fig. 1i, top), showing the greater sensitivity of cholinergic amacrine cells in the inner nuclear layer (INL) for this excitotoxic effect. Counts of cholinergic amacrine cells in such sectioned material confirmed the partial loss within the GCL, yet a near-complete ablation in the INL (Figs. 1l and 1m). This differential sensitivity was also recently reported in the developing rat retina (Chun et al., 2001). Counts of rod bipolar cells, or of glycinergic amacrine cells, showed no effect upon these cells (Figs. 1n and 1o).

Retinal ganglion cells, particularly the largest, alpha cells, and amacrine cells are well activated by the glutamate agonists kainate, AMPA and NMDA, and are known in other species to be susceptible to excitotoxic ablation by L-glutamate (Marc, 1999*a*,*b*; Reese et al., 2001; Johnson et al., 2001). Consequently, we also counted the number of large, darkly stained, neurofilament (150 kDa)-immunoreactive retinal ganglion cells, and GABAergic amacrine cells, and, like the cholinergic amacrine cells, found a conspicuous excitotoxic sensitivity (Figs. 1p and 1q). Their loss should contribute to the pronounced reduction in the thickness of the IPL observed in the above micrographs (Figs. 1h–1k).

These results show that L-glutamate can be used as an excitotoxic agent to eliminate cholinergic amacrine cells, but that this excitotoxicity is not selective. As found in the developing ferret's retina (Reese et al., 2001; Johnson et al., 2001), L-glutamate exposure also significantly reduces other amacrine cells as well as retinal ganglion cells, and so any changes within the inner retina must be interpreted accordingly. What, then, is the effect of partially reducing the population of cholinergic amacrine cells within the GCL upon the positioning of those that survive this excitotoxic insult?

Cholinergic mosaic organization

The spatial organization of the cholinergic amacrine cell mosaic in the adult mouse retina has been described in detail (Galli-Resta et al., 2000). We compared the mosaic organization of the cholinergic amacrine cell population in the GCL in eight saline-treated mice with that in three mice that had been exposed to 2.6 mg/g L-glutamate on P-3, which had produced an average reduction of 43% (Fig. 1f). Figs. 2a–2d show frequency distributions for four Voronoi-based measures of the geometry of the mosaic: the Delaunay segment lengths, being the distances between all Voronoi neighbors; the Delaunay triangle areas, being the areas of all triangles defined by the population of Delaunay segments; the nearest-neighbor distances, being the shortest Delaunay segment for each cell; and the Voronoi domains themselves, being the areas defined by the bisectors passing through each Delaunay segment (each Voronoi domain for a cell, therefore, is the area of all points in the field closer to that cell than to any other). All of these comparisons show that the distributions associated with the experimental condition are shifted to larger values, as would be expected if the population had been reduced in density.

If the depleted retinas are scaled to match the densities of the control retinas, and their distributions are then compared directly, they can be seen to superimpose modestly, consistent with the idea that the surviving cells have moved upon the retina to maintain the same spatial geometry as seen in the normal retina (Figs. 2e–2h), although close inspection shows relatively poorer fits for some of the comparisons. An alternative approach is to compare directly the regularity index, which is a scale-independent measure of the variability in each population, being the average nearest-neighbor distance divided by the standard deviation. If we compute this regularity index, we find an average for the cholinergic amacrine cells in the GCL in the control retina to be 3.27 ± 0.25 ($n = 30$ fields, drawn from three retinas), while that for the depleted retinas is lower, being 2.98 ± 0.22 ($n = 33$ fields, from three retinas). This difference appears modest, implying that despite a 40% reduction in the population of cholinergic amacrine cells, their mosaic properties do not appear to be conspicuously reduced.

As described by Cook (1996), however, the regularity index derived from nearest-neighbor analysis is relatively immune to undersampling. A mosaic with a regularity index of ~3.3 drops to

Fig. 1. Early L-glutamate treatment can be used to modulate the population of cholinergic amacrine cells. *a*: Subcutaneous injection of 4.0 mg/g L-glutamate on P-6 reduces the population of ChAT-immunopositive (+) amacrine cells in the GCL by 95%, assessed on P-24. *b*: Effects of treatment are age dependent: analysis of variance shows an effect of age of treatment ($p < 0.0001$) and *post-hoc* scheffe comparisons confirm differences at P-4 and P-6 *vs.* control (and *vs.* P-2) conditions ($p < 0.0001$), but no difference between the former two, nor between the control and P-2 treatment conditions. *c* & *d*: Effects are relatively selective for the cholinergic amacrine cells, as such injections do not affect the density of horizontal (Calb+) nor dopaminergic (TH+) amacrine cells ($p > 0.1$). *e*: Retinal area is slightly compromised following treatment at P-4 and P-6: analysis of variance shows an effect of age of treatment on retinal area ($p < 0.005$), and *post-hoc* scheffe comparisons confirm differences between control *vs.* treatment conditions at P-4 and P-6 ($p < 0.05$), but not between any of the three treatment groups, and nor between the P-2 and control groups. *f*: Effects of treatment are dose dependent: analysis of variance shows an effect of dosage at P-3 ($p < 0.0001$) and *post-hoc* scheffe comparisons confirm differences between every comparison ($p < 0.0001$) except between 1.3 *vs.* 2.6 mg/g treatment groups. *g*: Surviving cholinergic amacrine cells in the GCL show no change in soma area. *h*: Cytoarchitecture of the retina is normal at P-24 following treatment on P-3, although the inner retina is thinner. *i–k*: Lamination within the plexiform layers is also normal, evidenced by immunohistochemistry for the processes of ChAT-immunoreactive (+) cells, Calb+ horizontal cells, TH+ amacrine cells, PKC+ bipolar cells, GlyT1+ amacrine cells, GABAergic amacrine cells, and NF+ ganglion cells, although the thickness of IPL is reduced. Note the complete abolition of the cholinergic amacrine cells in the INL and their associated stratum within the IPL (top right of *i*); two remaining cholinergic amacrine cells in the GCL continue to stratify normally in the inner part of the IPL. *l* & *m*: Treatment on P-3 near-completely abolishes cholinergic cells in the INL ($p < 0.005$), while only partially reducing the population in the GCL ($p < 0.05$). *n* & *o*: Rod bipolar (PKC+) cells and glycinergic (GlyT1+) amacrine cells are not affected ($p > 0.1$). *p* & *q*: GABAergic amacrine cells in the INL are significantly affected, as are large, intensely stained, NF-immunopositive (150 kDa) ganglion cells in the GCL ($p < 0.05$; Student's *t*-tests with unequal variance in *l–q*). In each histogram, the number of retinas analyzed is indicated in each bar (or, in the case of *g*, the number of cells measured is indicated).

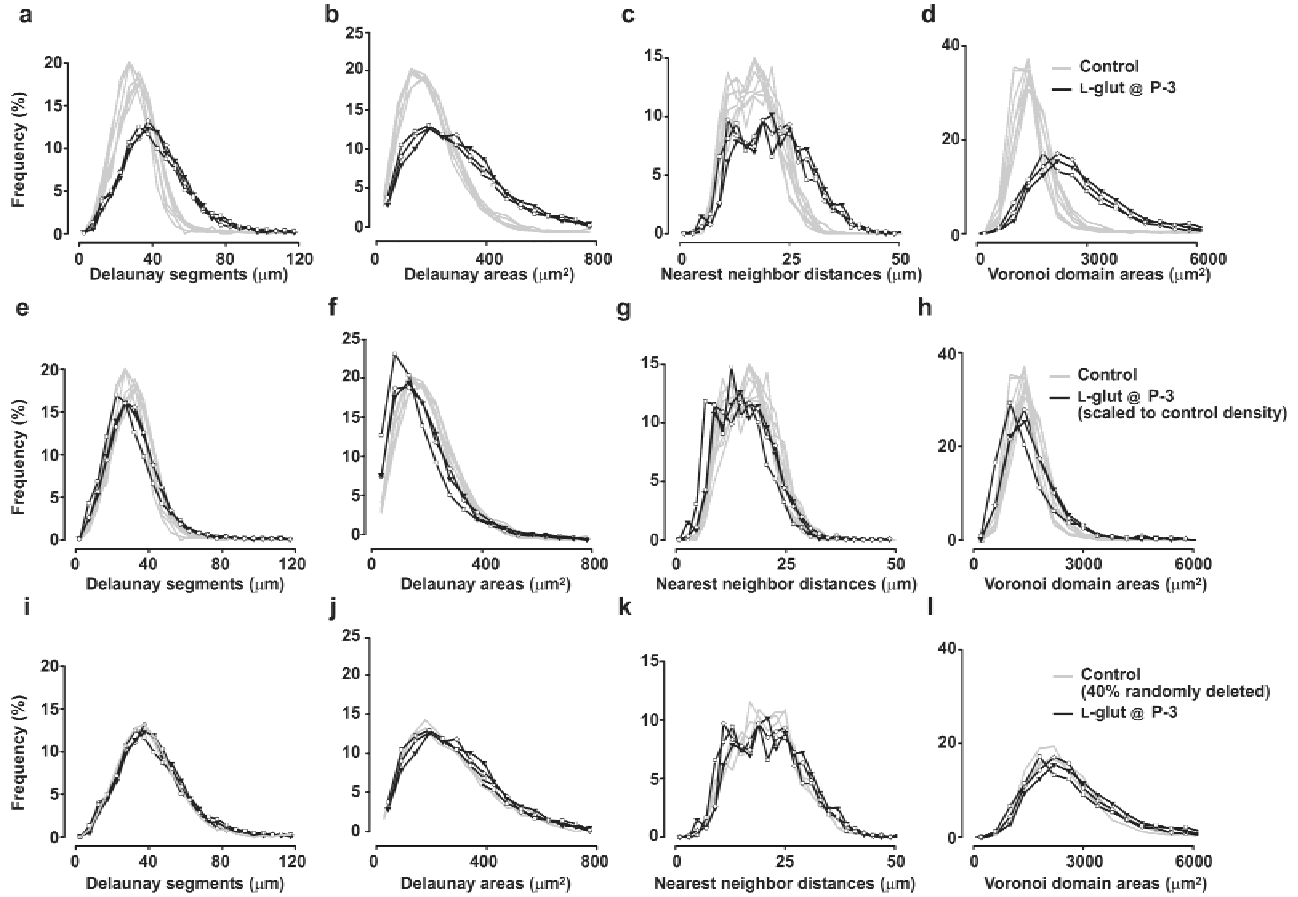

Fig. 2. Early partial elimination of cholinergic amacrine cells does not induce remaining cells to move tangentially to maintain uniform intercellular spacing. Each panel shows the average frequency distribution of individual saline-treated retinas or L-glutamate-treated retinas for their Delaunay segment lengths (*a*, *e*, *i*), Delaunay triangle areas (*b*, *f*, *j*), nearest-neighbor lengths (*c*, *g*, *h*) and Voronoi domain areas (*e*, *h*, *l*). *a–d*: Control mosaics (grey lines) compared with depleted mosaics (black lines and symbols) showing an average reduction of 40%. *e–h*: Control mosaics (same grey lines) are now compared with depleted mosaics (black lines and symbols) after the latter measures have been scaled by the ratio of their average densities, in order to compare more directly the shape of the distributions. *i–l*: Same data in figures *a–d* but with three of the control mosaics undergoing a random deletion of 40% (grey lines). Such a random elimination positions the normal mosaics within the population of experimentally depleted retinas (black lines and symbols) for all four measures.

about 2.9 when undersampled by about 40% (Cook, 1996). To examine this directly, we took three of the control retinas and randomly deleted cells from each of their fields by 40%, and then conducted the same analysis on the resultant mosaics (Figs. 2i–2l). Such distributions from randomly deleted mosaics generally fall within the envelop of the L-glutamate-treated distributions, and the regularity indexes derived from these randomly deleted mosaics now overlap exactly with the experimentally depleted ones, being 2.92 ± 0.21 ($n = 26$ of the above normal fields, followed by random 40% deletion). These results, then, suggest that a partial reduction in the amacrine cell mosaic by about 40%, induced on P-3, does not in any way alter the positioning of the surviving cholinergic amacrine cells.

Rather than shifting position on the retina to maintain a uniform spacing, perhaps cholinergic amacrine cells increase their dendritic field size following loss of their neighbors. Given that the area of the dendritic field of a cholinergic amacrine cell on P-3 is roughly one-seventh of its mature size (Stacy & Wong, 2003), but that retinal area increases during this same period by only a factor of 2–3, active dendritic growth may compensate for the reduction in density, thereby maintaining dendritic coverage (see also Wong & Collin, 1989). Does the size of a cholinergic amacrine cell's dendritic field change following partial elimination of its neighboring cells?

Cholinergic dendritic field size

The "starburst" morphology that is characteristic of cholinergic amacrine cells in other species is also known to be present in the mouse retina (Badea et al., 2003). These cells, in the GCL, exhibit ~5–7 primary dendrites radiating within the inner (or ON) stratum within the IPL. Those dendrites branch into secondary and then higher order dendrites that continue to run primarily radially, showing little cross-over with one another (Fig. 3a). The central dendrites show occasional spines and varicosities, while the more peripheral dendrites are studded with prominent varicosities defining an annulus (Fig. 3d). Dendritic field area varies conspicuously, as it does in the rat retina (Voigt, 1986), but regression analysis

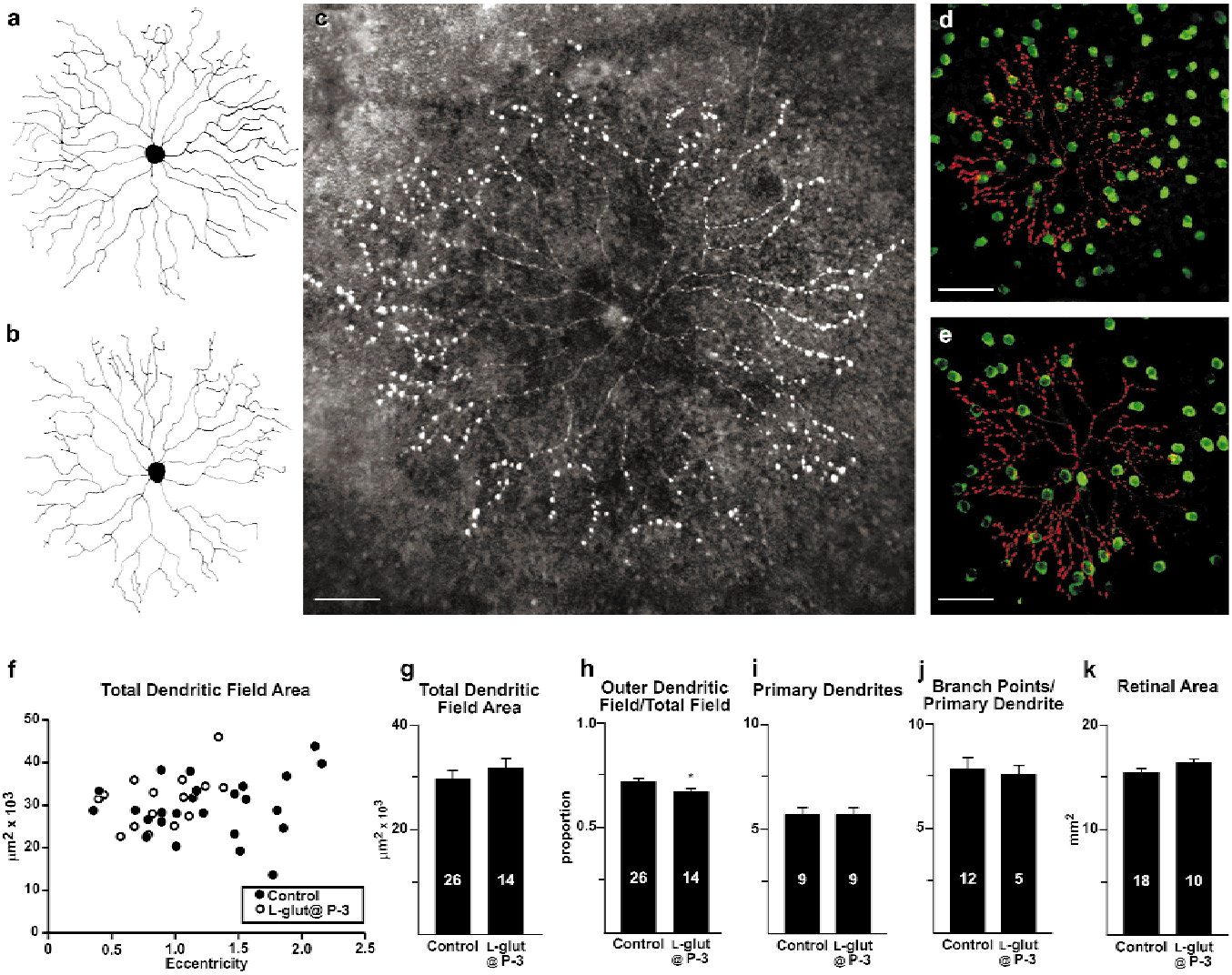

Fig. 3. Dendritic fields of surviving cholinergic amacrine cells do not grow compensatorily following the partial elimination of neighboring processes. *a* & *b*: Drawings of Lucifer Yellow (LY) labeled amacrine cells, showing a classic starburst morphology, in both normal (*a*) and treated (*b*) retina. *c*: Varicose-rich distal dendrites define an annulus within the dendritic field, characteristic of starburst amacrine cells in other species, even in cells from treated retinas (shown here). Calibration bar = 25 μm. *d* & *e*: Confocal images of filled cells (red) in normal (*d*) and treated (*e*) retinas, and the surrounding population of cholinergic amacrine cells (green). There are 42% fewer cholinergic amacrine cells in field *e* relative to *d*. The number underlying each dendritic field equals 36 (in *d*) and 24 (in *e*). Calibration bar = 50μm. Figs. *a–e* also show the variation in starburst morphology, being not obviously greater amongst the population of cells within treated retinas. The confocal stacks in *d* and *e* have excluded the planes containing the anti-LY labeled (red) soma. The LY-labeled somata drawn in *a* and *b* are an overestimation, as the drawings were made from fluorescence micrographs collected in the IPL. The somata in the GCL give rise to a single dendrite that yields 5–7 primary branches within the IPL. *f*: Total dendritic field area does not increase in size with retinal eccentricity. *g*: Total dendritic field area is slightly (though not significantly) larger in treated retinas. *h*: The inner dendritic field area defined by the annulus is slightly larger in cells from treated retinas, while the annular field area did not differ, rendering the annulus to be 5% smaller, as a proportion of total dendritic field area ($p < 0.05$; *t*-test). *i*: The number of primary radiating dendrites was the same in cells from normal and treated retinas. *j*: The frequency of branch-points downstream from a primary dendrite did not differ. *k*: Retinal area did not differ between these L-glutamate-treated and normal retinas. In each histogram, the number of cells analyzed is indicated in each bar (or, in *k*, the number of retinas from which these cells were harvested is indicated).

indicates no significant change with eccentricity (Fig. 3f). The average dendritic field area for the population of 26 cholinergic cells from normal retinas was 29,360 μm^2 (being a diameter of 193 μm), while the outer portion (or annulus) of the field rich in terminal and *en passant* varicosities was 21,078 μm^2, and the inner portion defined by that annulus was 8283 μm^2.

Following 2.6 mg/g L-glutamate on P-3, filled cells with a starburst morphology were still present (Figs. 3b, 3c and 3e). These cells showed the morphological characteristics of starburst cells in the normal retina, including discriminable inner/outer compartments in the dendritic field (Fig. 3c). These 14 cells, when compared with those from normal retinas, showed a slight but not

significant increase in total dendritic area of 31,653 μm^2 (or a diameter of 200 μm; Fig. 3g), and a small increase in the inner, but not the outer, dendritic field compartments, rendering a 5% decrease in the proportion of dendritic field area occupied by the varicose-rich annulus (Fig. 3h). While there was some variation in the symmetry of the organization of the dendritic field (Fig. 3e), such asymmetries were seen amongst the cells from untreated retinas as well (Fig. 3d). They exhibited no difference in their number of primary dendrites (Fig. 3i) nor in the frequency of downstream branch-points associated with primary dendrites (Fig. 3j). They were strikingly similar, and provided no other obvious cue to discriminating them when compared "blind." When compared with the pattern of depleted cells, no obvious nor consistent local morphological changes were apparent (Fig. 3e). The population of cells from treated retinas came from the central 1.5 mm of retina, whereas the normal population extended to further eccentricities (Fig. 3f); excluding these ten further eccentric cells from the normal sample did not alter the results of the statistical comparisons.

Given the average size of the dendritic field for cholinergic amacrine cells, we can estimate, for the mouse, the normal dendritic coverage for this population (Fig. 3d). The average size of the retinas contributing this sample of 40 cells was 15.7 mm^2 ($n = 28$), with a slight, if nonsignificant increase in the size of the L-glutamate-treated retinas (Fig. 3k). As cholinergic cell density had been determined in three-week-old mice (Fig. 1f), those retinas had not yet grown to full size, being on average only 11.93 mm^2. (Note that all of the cholinergic amacrine cells are ChAT-immunoreactive at this time, as estimating the total number per retina at this age yields counts of ~17,000 cells, being comparable to other estimates of both ON and OFF cholinergic amacrine cells in the mouse retina (Jeon et al., 1998; Galli-Resta, 2000; Strettoi & Volpini, 2002). Consequently, we need to scale the average density of 1466 cells/mm^2 at 3 weeks of age accordingly, to 1111 cells/mm^2. Using this value, which is slightly greater than the average of 945 cells/mm^2 reported elsewhere (Jeon et al., 1998), the average dendritic coverage for cholinergic amacrine cells in the normal mouse retina is therefore 33 (or 28 if we use the average estimated density from Jeon et al., 1998). This coverage factor is greater than that observed in the rat retina, being around 20, due to the lower density of cholinergic amacrine cells therein (Voigt, 1986). For the L-glutamate-treated mice, their total dendritic field area of 31,653 μm^2 yields an average dendritic coverage factor of only 20, indicating that the slight (and nonsignificant) increase in total dendritic field area of surviving cholinergic amacrine cells (Fig. 3g) does not come close to providing the coverage observed in the normal mouse retina. In fact, this coverage factor is reduced by 40% relative to normal, indicating no compensatory increase following partial ablation whatsoever (Fig. 3e).

Discussion

The present results demonstrate three main findings: First, we have defined the effectiveness of L-glutamate as an excitotoxin to kill developing cholinergic amacrine cells. Second, using this approach, we have shown that remaining cholinergic amacrine cells do not redistribute themselves on the retina following partial ablation of their neighbors. And third, we have demonstrated that they do not exhibit any compensatory growth in dendritic field size following depletion of the local cholinergic plexus.

The use of L-glutamate as an excitotoxin for cholinergic amacrine cells

L-glutamate and its analogues have been established as effective excitotoxins in the developing mouse retina (Olney, 1969; Olney et al., 1971), and have been shown to deplete the population of cholinergic amacrine cells in the developing chick, rat, and ferret retina (Karlsen, 1978; Fischer et al., 1998; Reese et al., 2001; Johnson et al., 2001). The present study confirms this relative selectivity in the mouse retina. It also shows, however, that GABAergic amacrine cells are also severely depleted, as are the larger retinal ganglion cells. This vulnerability of GABAergic neurons has been previously reported in the mouse (Yoon et al., 1999), and the sensitivity of the largest ganglion cells was reported for the ferret (Reese et al., 2001). This spectrum of excitotoxic action should be due to ionotropic glutamate receptor expression across different cell types, and to their different developmental profiles (Zhang et al., 1996). For example, the lack of excitotoxic action prior to P-3 most likely reflects the onset of receptor expression in cholinergic amacrine cells around this time, while the lack of any effect upon the horizontal cells at the times examined may be indicative of the later maturation of synaptic connectivity in the outer retina, at the close of the first postnatal week (Olney, 1968; Kapfhammer et al., 1994; West Greenlee et al., 1996; Dhingra et al., 1997; Rich et al., 1997). A preliminary report from a recent study in developing rat retina indicates a similar spectrum of vulnerability, with cholinergic and GABAergic amacrine cells being severely depleted, while horizontal cells, glycinergic amacrine cells, and dopaminergic amacrine cells being immune to the excitotoxicity (Chun et al., 2001).

Mosaic organization

Cholinergic amacrine cells disperse tangentially during development, and their mosaic geometry is maintained while later-arriving cells migrate into the mosaic layer (Galli-Resta et al., 1997; Reese et al., 1999). Furthermore, when their microtubules are destabilized, the emerging cholinergic mosaic becomes disorderly, reestablishing their order after microtubule stability is regained (Galli-Resta et al., 2002). We reasoned, therefore, that partially depleting the cholinergic amacrine cells during development might lead to a reestablishment of their mosaic regularity as these cells undergo interactions with their next-nearest (remaining) neighbors following ablation, spacing themselves out accordingly. We failed to find any evidence for such regulation. The lack of such regulation does not appear to be due to any toxic effect of the L-glutamate directly upon the surviving cells, since they have been sufficiently healthy to grow and achieve a normal starburst morphology. An alternative expectation was that, should the cholinergic amacrine cells exert a tensile force upon one another that contributes to their regularity (Galli-Resta, 2002), perturbing the micromechanical equilibrium through this partial ablation might degrade the mosaic, as observed transiently following microtubule destabilization (Galli-Resta et al., 2002). Yet no evidence was found for this either, the final mosaic being exactly predicted from a random 40% deletion from the normal mosaic.

The microtubule destabilization studies were conducted in rats on the day of birth, whereas partial cholinergic ablation in mice could not be produced using L-glutamate prior to P-3. Excitotoxic cell death is rapid, with immature cholinergic amacrine cells in the ferret's retina presenting a fragmented appearance after 1 h, and being eliminated within 24 h (Reese et al., 2001), so the depletion

in mouse retina should be established shortly after L-glutamate exposure. Note that this is still at a stage during development when the primary dendrites radiate directly from the cholinergic amacrine cell somata; as the IPL subsequently increases in thickness, the somata become displaced from their stratifying processes in the IPL (Kim et al., 2000; Stacy & Wong, 2003). Perhaps this is still too late to achieve an alteration in neighbor relationships that influences tangential dispersion. However, P-4 cholinergic amacrine cells in the mouse retina undergo a seven-fold expansion in their dendritic field area by adulthood (Stacy & Wong, 2003; present results), while retinal area only triples, at most, during this period, so dynamic dendritic growth (including process addition as well as elimination, elongation as well as shortening) should still be occurring after the period of partial cholinergic ablation (Wong & Wong, 2000). The latter may simply be insufficient to influence somal positioning after the rudimentary architecture of the cholinergic amacrine cell has been established (Wong & Collin, 1989; Stacy & Wong, 2003).

Dendritic coverage

The present results also demonstrate this subsequent growth of cholinergic dendrites is not controlled by the density of neighboring processes. A 40% reduction in the density of cholinergic amacrine cells and their processes is not sufficient to produce an enhanced growth of developing dendrites leading to a larger total dendritic area, or to a greater density of dendrites, inferred by there being no change in the number of primary dendrites nor in the number of branch-points arising from a primary dendrite. Morphologically, these cells display the characteristics of the classic starburst appearance, and are qualitatively indistinguishable from those in normal retinas. The cause of the small reduction in the proportion of the dendritic field area devoted to the varicosity-rich annulus is not clear. Whatever the explanation for this difference, there is no escaping the conclusion that dendritic growth of cholinergic amacrine cells is not finely tuned by the local density of cholinergic processes. This absence of an effect is not for lack of opportunity to interact, as their processes normally fasciculate within their respective strata in the IPL where they also exchange synaptic contacts (Tauchi & Masland, 1985; Brandon, 1987; Millar & Morgan, 1987). We cannot rule out the possibilities that there is some threshold density triggering an upper limit on dendritic field size (i.e. greater depletions might have shown a compensatory increase), nor that supernormal densities might reduce dendritic field size, but the present results suggest that, once a cholinergic cell has begun to differentiate, the size of its dendritic field is controlled by cell-intrinsic factors; further interstitial growth associated with differential retinal expansion may then increase this density-independent regulation of field size (Rodieck & Marshak, 1992). While synaptic relationships with bipolar terminals and ganglion cell dendrites undoubtedly play a shaping role in other aspects of the cholinergic amacrine cell's dendritic structure, it is difficult to see how they may influence the overall size of the dendritic field.

The unchanging behavior of cholinergic amacrine cells in the absence of local homotypic neighbors is to be contrasted with that of retinal ganglion cells, redirecting their differentiating dendrites into regions that have been locally depleted (Perry & Linden, 1982; Eysel et al., 1985). As mentioned above, these two cell types show a greater than ten-fold difference in their dendritic coverage factors (Wässle et al., 1981*a*,*b*), with some retinal ganglion cells having a coverage factor of just 1 (Amthor & Oyster, 1995). To achieve the latter, dendrites of neighboring cells may experience a homotypic contact inhibition of further growth. Cholinergic amacrine cells, by contrast, may have their dendritic fields determined by cell-intrinsic constraints, being ignorant of local homotypic processes. A parallel arrangement was recently described for *Drosophila* sensory neurons, in which one type of cell, providing a uniform coverage of the body wall with nonoverlapping dendrites, was found to increase or decrease their dendritic field in response to laser ablation or genetic addition of homotypic cells, respectively. Other types of sensory cells, that under normal conditions do not provide the same uniform nonoverlapping dendritic coverage, were found to overlap extensively when their numbers were increased through genetic manipulation of fate (Grueber et al., 2003). These studies indicate that the constraints upon dendritic growth for different types of cell are quite distinct, even for cell types inhabiting the same local milieu.

Acknowledgments

This research was supported by a grant from the National Institutes of Health (EY11087). We thank Brian Necessary for assistance with preliminary studies on L-glutamate excitotoxicity, and Lucia Galli-Resta for assistance with mosaic analysis.

References

Amthor, F.R. & Oyster, C.W. (1995). Spatial organization of retinal information about the direction of image motion. *Proceedings of the National Academy of Sciences of the U.S.A.* **92**, 4002–4005.

Ault, S.J., Thompson, K.G., Zhou, Y. & Leventhal, A.G. (1993). Selective depletion of beta cells affects the development of alpha cells in cat retina. *Visual Neuroscience* **10**, 237–245.

Badea, T.C., Wang, Y. & Nathans, J. (2003). A noninvasive genetic/pharmacologic strategy for visualizing cell morphology and clonal relationships in the mouse. *Journal of Neuroscience* **23**, 2314–2322.

Brandon, C. (1987). Cholinergic neruons in the rabbit retina: Dendritic branching and ultrastructural connectivity. *Brain Research* **426**, 119–130.

Chun, M.-H., Park, S.-J., Kim, I.-B., Moon, H.-I., Kang, W.-S., Oh, S.-J. & Chung, J.-W. (2001). Excessive L-glutamate induces selective neuronal death in the developing rat retina. *Association for Research in Vision and Ophthalmology Abstracts* **42**, 4013.

Cook, J.E. (1996). Spatial properties of retinal mosaics: An empirical evaluation of some existing measures. *Visual Neuroscience* **13**, 15–30.

Deplano, S., Gargini, C. & Bisti, S. (1999). Electrical activity regulates dendritic reorganization in ganglion cells after neonatal retinal lesion in the cat. *Journal of Comparative Neurology* **405**, 262–270.

Dhingra, N.K., Ramamohan, Y. & Raju, T.R. (1997). Developmental expression of synaptophysin, synapsin I and syntaxin in the rat retina. *Developmental Brain Research* **102**, 267–273.

Eglen, S.J., van Ooyen, A. & Willshaw, D.J. (2000). Lateral cell movement driven by dendritic interactions is sufficient to form retinal mosaics. *Network: Computation in Neural Systems* **11**, 103–118.

Eysel, U.T., Peichl, L. & Wässle, H. (1985). Dendritic plasticity in the early postnatal feline retina: Quantitative characteristics and sensitive period. *Journal of Comparative Neurology* **242**, 134–145.

Famiglietti, E.V. (1983). "Starburst" amacrine cells and cholinergic neurons: Mirror-symmetric ON and OFF amacrine cells of rabbit retina. *Brain Research* **261**, 138–144.

Famiglietti, E.V. (1991). Synaptic organization of starburst amacrine cells in rabbit retina: Analysis of serial thin sections by electron microscopy and graphic reconstruction. *Journal of Comparative Neurology* **309**, 40–70.

Fischer, A.J., Pickett Seltner, R.L., Poon, J. & Stell, W.K. (1998). Immunocytochemical characterization of quisqualic acid- and N-methyl-D-aspartate-induced excitotoxicity in the retina of chicks. *Journal of Comparative Neurology* **393**, 1–15.

Galli-Resta, L. (2000). Local, possibly contact-mediated signalling restricted to homotypic neurons controls the regular spacing of cells within the cholinergic arrays in the developing rodent retina. *Development* **127**, 1509–1516.

Galli-Resta, L. (2002). Putting neurons in the right places: Local interactions in the genesis of retinal architecture. *Trends in Neurosciences* **25**, 638–643.

Galli-Resta, L., Resta, G., Tan, S.-S. & Reese, B.E. (1997). Mosaics of islet-1 expressing amacrine cells assembled by short range cellular interactions. *Journal of Neuroscience* **17**, 7831–7838.

Galli-Resta, L., Novelli, E., Volpini, M. & Strettoi, E. (2000). The spatial organization of cholinergic mosaics in the adult mouse retina. *European Journal of Neuroscience* **12**, 3819–3822.

Galli-Resta, L., Novelli, E. & Viegi, A. (2002). Dynamic microtubule-dependent interactions position homotypic neurones in regular monolayered arrays during retinal development. *Development* **129**, 3803–3814.

Grueber, W.B., Ye, B., Moore, A.W., Jan, L.Y. & Jan, Y.N. (2003). Dendrites of distinct classes of *Drosophila* sensory neurons show different capacities for homotypic repulsion. *Current Biology* **13**, 618–626.

He, S., Weiler, R. & Vaney, D.I. (2000). Endogenous dopaminergic regulation of horizontal cell coupling in the mammalian retina. *Journal of Comparative Neurology* **418**, 33–40.

Honjo, M., Tanihara, H., Suzuki, S., Tanaka, T., Honda, Y. & Takeichi, M. (2000). Differential expression of cadherin adhesion receptors in neural retina of the postnatal mouse. *Investigative Ophthalmology and Visual Science* **41**, 546–551.

Jeon, C.-J., Strettoi, E. & Masland, R.H. (1998). The major cell populations of the mouse retina. *Journal of Neuroscience* **18**, 8936–8946.

Johnson, P.T., Raven, M.A. & Reese, B.E. (2001). Disruption of transient photoreceptor targeting within the inner plexiform layer following early ablation of cholinergic amacrine cells in the ferret. *Visual Neuroscience* **18**, 741–751.

Kapfhammer, J.P., Christ, F. & Schwab, M.E. (1994). The expression of GAP-43 and synaptophysin in the developing rat retina. *Developmental Brain Research* **80**, 251–260.

Karlsen, R.L. (1978). The toxic effect of sodium glutamate and DL-alpha-aminoadipic acid on rat retina: Changes in high affinity uptake of putative transmitters. *Journal of Neurochemistry* **31**, 1055–1061.

Kim, I.-B., Lee, E.-J., Kim, M.-K., Park, D.-K. & Chun, M.-H. (2000). Choline acetyltransferase-immunoreactive neurons in the developing rat retina. *Journal of Comparative Neurology* **427**, 604–616.

Linden, R. & Perry, V.H. (1982). Ganglion cell death within the developing retina: A regulatory role for retinal dendrites? *Neuroscience* **7**, 2813–2837.

Lohmann, C. & Wong, R.O.L. (2001). Cell-type specific dendritic contacts between retinal ganglion cells during development. *Journal of Neurobiology* **48**, 150–162.

Lohmann, C., Myhr, K.L. & Wong, R.O. (2002). Transmitter-evoked local calcium release stabilizes developing dendrites. *Nature* **418**, 177–181.

Marc, R. (1999*a*). Mapping glutamatergic drive in the vertebrate retina with a channel-permeant organic cation. *Journal of Comparative Neurology* **407**, 47–64.

Marc, R. (1999*b*). Kainate activation of horizontal, bipolar, amacrine, and ganglion cells in the rabbit retina. *Journal of Comparative Neurology* **407**, 65–76.

Millar, T.J. & Morgan, I.G. (1987). Cholinergic amacrine cells in the rabbit retina synapse onto other cholinergic amacrine cells. *Neuroscience Letters* **74**, 281–285.

Olney, J.W. (1968). An electron microscopic study of synapse formation, receptor outer segment development, and other aspects of developing mouse retina. *Investigative Ophthalmology* **7**, 250–268.

Olney, J.W. (1969). Glutamate-induced retinal degeneration in neonatal mice. Electron mocroscopy of the acutely evolving lesion. *Journal of Neuropathology and Experimental Neurology* **28**, 455–474.

Olney, J.W., Ho, O.L. & Rhee, V. (1971). Cytotoxic effects of acidic and sulphur containing amino acids on the infant mouse central nervous system. *Experimental Brain Research* **14**, 61–76.

Park, J.-J., Oh, S.-J., Chung, J.-W. & Chun, M.-H. (2002). Tolerance of horizontal cells to excitotoxicity in the developing FVB/N mouse retina. *NeuroReport* **13**, 2091–2095.

Perry, V.H. & Linden, R. (1982). Evidence for dendritic competition in the developing retina. *Nature* **297**, 683–685.

Raven, M.A. & Reese, B.E. (2002). Horizontal cell density and mosaic regularity in pigmented and albino mouse retina. *Journal of Comparative Neurology* **454**, 168–176.

Reese, B.E. & Galli-Resta, L. (2002). The role of tangential dispersion in retinal mosaic formation. *Progress in Retinal and Eye Research* **21**, 153–168.

Reese, B.E., Necessary, B.D., Tam, P.P.L., Faulkner-Jones, B. & Tan, S.-S. (1999). Clonal expansion and cell dispersion in the developing mouse retina. *European Journal of Neuroscience* **11**, 2965–2978.

Reese, B.E., Raven, M.A., Giannotti, K.A. & Johnson, P.T. (2001). Development of cholinergic amacrine cell stratification in the ferret retina and the effects of early excitotoxic ablation. *Visual Neuroscience* **18**, 559–570.

Rich, K.A., Zhan, Y. & Blanks, J.C. (1997). Migration and synaptogenesis of cone photoreceptors in the developing mouse retina. *Journal of Comparative Neurology* **388**, 47–63.

Rodieck, R.W. & Marshak, D.W. (1992). Spatial density and distribution of choline acetyltransferase immunoreactive cells in human, macaque, and baboon retinas. *Journal of Comparative Neurology* **321**, 46–64.

Rossi, C., Strettoi, E. & Galli-Resta, L. (2003). The spatial order of horizontal cells is not affected by massive alterations in the organization of other retinal cells. *Journal of Neuroscience* **23**, 9924–9928.

Sandmann, D., Engelmann, R. & Peichl, L. (1997). Starburst cholinergic amacrine cells in the tree shrew retina. *Journal of Comparative Neurology* **389**, 161–176.

Schmidt, M., Wässle, H. & Humphrey, M. (1985). Number and distribution of putative cholinergic amacrine cells in cat retina. *Neuroscience Letters* **59**, 235–240.

Stacy, R.C. & Wong, R.O.L. (2003). Developmental relationship between cholinergic amacrine cell processes and ganglion cell dendrites of the mouse retina. *Journal of Comparative Neurology* **456**, 154–166.

Strettoi, E. & Volpini, M. (2002). Retinal organization in the bcl-2-overexpressing transgenic mouse. *Journal of Comparative Neurology* **446**, 1–10.

Tauchi, M. & Masland, R.H. (1984). The shape and arrangement of the cholinergic neurons in the rabbit retina. *Proceedings of the Royal Society B* (London) **223**, 101–119.

Tauchi, M. & Masland, R.H. (1985). Local order among the dendrites of an amacrine cell population. *Journal of Neuroscience* **5**, 2494–2501.

Vaney, D.I. (1984). "Coronate" amacrine cells in the rabbit retina have the "starburst" dendritic morphology. *Proceedings of the Royal Society B* (London) **220**, 501–508.

Voigt, T. (1986). Cholinergic amacrine cells in the rat retina. *Journal of Comparative Neurology* **248**, 19–35.

Wässle, H. & Riemann, H.J. (1978). The mosaic of nerve cells in the mammalian retina. *Proceedings of the Royal Society B* (London) **200**, 441–461.

Wässle, H., Boycott, B.B. & Illing, R.-B. (1981*a*). Morphology and mosaic of on- and off-beta cells in the cat retina and some functional considerations. *Proceedings of the Royal Society B* (London) **212**, 177–195.

Wässle, H., Peichl, L. & Boycott, B.B. (1981*b*). Morphology and topography of on- and off-alpha cells in the cat retina. *Proceedings of the Royal Society B* (London) **212**, 157–175.

West Greenlee, M.H., Swanson, J.J., Simon, J.J., Elmquist, J.K., Jacobson, C.D. & Sakaguchi, D.S. (1996). Postnatal development and the differential expression of presynaptic terminal-associated proteins in the developing retina of the Brazilian opossum, *Monodelphis domestica*. *Developmental Brain Research* **96**, 159–172.

Wong, R.O.L. & Collin, S.P. (1989). Dendritic maturation of displaced putative cholinergic amacrine cells in the rabbit retina. *Journal of Comparative Neurology* **287**, 164–178.

Wong, R.O.L. & Ghosh, A. (2002). Activity-dependent regulation of dendritic growth and patterning. *Nature Reviews Neuroscience* **3**, 803–812.

Wong, W.T. & Wong, R.O. (2000). Rapid dendritic movements during synapse formation and rearrangement. *Current Opinion in Neurobiology* **10**, 118–124.

Yoon, Y.H., Jeong, K.H., Shim, M.J. & Koh, J.Y. (1999). High vulnerability of GABA-immunoreactive neurons to kainate in rat retinal cultures: Correlation with the kainate-stimulated cobalt uptake. *Brain Research* **823**, 33–41.

Zhang, C., Hammassaki-Britto, D.E., Britto, L.R.G. & Duvoisin, R.M. (1996). Expression of glutamate receptor subunit genes during development of the mouse retina. *NeuroReport* **8**, 335–340.